SUPPLEMENTAL MATERIAL

Detailed Methods and Results

Feature selection for supervised learning

An overview of MAP recording feature selection process is shown in Online Figure III. After cropping of the raw signals, each MAP recording was analyzed using the Python *tsfresh* library (Reference 20) Using this package, we calculated the complete library output available for signals of this size. This resulted in N = 794 scalar variables representing the mathematical features provided by the *tsfresh* library. This has been shown to effectively filter noise in time series signals and improve computational efficiency . We then used the Benjamini-Yekutieli approach (Reference 21), which can be applied to multiple tests to minimize the false discovery rate, assuming arbitrary dependence of p-values to select features most strongly linked with the outcomes (N = 622 [VT/VF] and N = 549 [Mortality]). Next, we dropped features that correlated highly to others to reduce redundancy left N=274 and N=259 features for each endpoint, respectively. Finally, the N = 40 features with highest coefficients for each endpoint were selected using logistic regression with L1 regularization and provided optimal performance of SVM in training.

Feature quantity analysis for supervised learning:

We performed an optimization analysis to determine the number of features used to generate the beat-level model. The top N features from the output of the tsfresh and logistic regression steps (Online Figure III) were used in iteratively training the SVM beat-level model. N

was ranged widely between 5 and 100 features with the resulting validation accuracy optimization curve. The optimal number of features was 40.

Supervised learning implementation using Support Vector Machine classifier:

For beat-level predictions, we compared several ML approaches including support vector machines (SVM), convolutional neural networks, and other supervised architectures. Extensive testing revealed that SVM classifier provided superior test characteristics to CNN (Online Table I and II).

The inputs (support vectors) were the scalar parameters from the output of the *tsfresh* output features described above. The SVM algorithm identifies a subset of inputs, termed support vectors, that form a decision boundary which optimally should separate output classes (endpoints). Training aims to increase the distance between input data and boundaries to improve the generalizability of the model. The supervised learning model was developed in Python 3.6. The Support Vector Machine classifier was implemented using sklearn library (scikit-learn 0.21.3). We used an SVM classifier (using "from sklearn.svm import SVC") with a linear kernel. To avoid overfitting in the SVM classifier, we trained the SVM classifier in 10-fold cross-validation using a regularization parameter of C = 1.

Supervised learning implementation using a convolutional neural network classifier:

The Convolutional Neural Network was implemented using tensorflow 2.1.0 and Keras 2.2.4-tf framework and written in Python 3.6. The raw voltage-time series data points from each MAP beat were directly used as inputs to the CNN (in contrast to feature outputs from the *tsfresh*

and logistic regression process). Training and testing were performed using the same K-fold cross validation splits discussed in the methods section for both analyses. The CNN architecture was implemented according to the architecture below, illustrated in Online Figure IV.

MAP score calculation and receiver operator characteristics analysis.

We developed the MAP score to generate a continuous patient-level index of risk for clinical outcomes from the output of the beat-level model. This allows all beats collected in a patient to be unified into a single risk prediction index despite biological or technical variability between beats. The MAP score is defined as the proportion of test set beats recorded from each patient that predict the endpoint of interest by the beat-level model. The proportion is calculated as:

$$\text{MAP score} = \left(\frac{\#\ of\ beats\ predicting\ the\ endpoint}{total\ \#\ of\ beats}\right)$$

for each endpoint in turn. For example, a patient in whom 80% of beat-level MAP recordings predicted VT/VF would be assigned a MAP score of 80%.

The ROC curve analysis was conducted in IBM SPSS v.19 by varying the cut-point of the MAP score from 0% to 100%. The output includes the data points used to draw the curves. These were imported into Jandel SigmaPlot version 11.0 which was used for graphing with better appearance.

Phase 1 repolarization analysis

We quantified phase 1 as the mean voltage of each MAP from the upstroke to dome of phase II, between 10 ms to 40 ms after phase 0. For MAP beats that predicted mortality, the

mean Phase 1 standardized voltage was lower than in those predicting survival (2.44 ± 1.31 vs. 3.32 ± 2.47, $p < 0.001$). This phase 1 metric predicted mortality with a c-statistic of 0.816 (CI: 0.676 to 0.957).

Biophysical simulation of MAPs classified by machine learning to predict each endpoint

We simulated cardiac cellular electrophysiology (membrane action potentials) using the O'Hara Rudy model, which has been validated in human ventricles and recommended by the FDA for drug testing for sudden cardiac death as part of the CiPa initiative (Reference 23). Cellular transmembrane action potentials were simulated following 160-beat stimulus train at 109 beats/min (550ms cycle length) to reach steady state. Two additional stimuli were applied at the same cycle length (550ms) and the action potential durations (APDs) of these extrastimuli were measured. APD measurements (APD_{XX}) were made in standard fashion by computing difference in time from the pacing stimulus (maximum time derivative of the tracing) and the time where the amplitude of the normalized tracing falls below 100% – XX% (where XX = 30 for APD30, 60 for APD60, and 90 for APD90). All waveforms were voltage-normalized across the dataset. If the difference between the APD90 of the first and second extrastimuli was greater than 50 ms, the case was marked as "APD alternans" and excluded from our analysis of steady-state action potential shapes.

The O'Hara model represents 14 transmembrane and 2 intracellular ion channels, pumps, and exchangers, referred to as ionic pathways, which we used to study action potential shapes. We focused on the hERG channel (IKr), L-Type Ca2+ Channel (ICaL), Na+-Ca2+ exchanger (NCX), Transient Outward current (Ito) and the sarcoplasmic reticulum ATPase

(SERCA), which have been reported to be the most important ionic pathways altered in heart failure (Reference 24). To identify the ionic pathways that may explain clinically measured MAP morphologies, we performed an extensive grid search. While computationally expensive, this method provides a global analysis with known accuracy. Of note, MAP measurements are recorded from patients with extensive cardiac disease and may not be well represented by the reference published ion pathway densities.

We consider that the densities of Ito, ICaL, IKr, NCX and SERCA could be altered under pathological conditions over a range of -80% to +100% for each ionic pathway, consistent with previous reported ranges used to model heart failure in humans (Reference 24). Parameter ranges for each channel are reported below (Online Methods Table 1). We separated each parameter range into 21 evenly spaced intervals and evaluate every parameter value permutation for all 5 ionic pathways. This results in 21^5 or 4,084,101 cell model parameter sets.

	Ito (Gto)	Ikr (GKr)	ICaL (pCa)	NCX (Gncx)	SERCA (JupMAX)
Min	0.004	0.0092	$0.2e^{-4}$	0.00016	0.000875
Max	0.04	0.092	$2e^{-4}$	0.0016	0.00875
Number of values	21	21	21	21	21

Online Methods Table 1. Ionic pathway, labelled by channel, exchanger and pump name and corresponding cell model parameter in brackets, ranges consider spanning -80% to +100% of reference values.

Simulations were performed for both mortality and VT/VF endpoints. For each, MAP traces representing the average trace for the event and non-event groups were used to explain the model parameter outputs. The best fit was determined based on smallest discrepancy

between APD30, 60, and 90 between event and non-event groups and between the spectrum of the measured and simulated tracings as described below.

MAP fitting by APD_{XX} and signal spectrum:

1. We define the set S_1 of the candidates satisfying the following conditions for **all** the APD_{XX}:

$$\frac{\left|APD_{XX}^{computed} - \mathbb{E}\left(APD_{XX}^{measured}\right)\right|}{\mathbb{S}\left(APD_{XX}^{measured}\right)} < C_{XX}$$

Here $\mathbb{E}\left(APD_{XX}^{measured}\right)$ is the APD_{XX} of the measured mean trace, $\mathbb{S}\left(APD_{XX}^{measured}\right)$ is the estimated APD_{XX} standard deviation and C_{XX} is a coefficient that prescribes a tolerance for APD_{XX}. We chose $C_{XX} = 1$ for all the APD_{XX}. This results in all simulated APDs from plausible parameter sets falling within one standard deviation of all measured APD.

2. In the second step, we associate each candidate $s_1^j \in S_1$ with the cost $\mathcal{C}\left(s_1^j\right)$ evaluated using the modal coefficients of the semi-classical signal analysis ($\mathcal{S}(s_1^j)$; see Signal Spectral Fit below) and the fit of the simulated to measured APD values. We build the set $S_2 \subset S_1$ of the candidates that satisfy:

$$\mathcal{C}\left(s_1^j\right) = \mathcal{S}\left(s_1^j\right) + \sum_{XX} \frac{\left|APD_{XX}^{computed} - \mathbb{E}\left(APD_{XX}^{measured}\right)\right|}{\mathbb{S}\left(APD_{XX}^{measured}\right)}$$

We adopt a 1% cut-off on $\mathcal{C}(s_1^j)$, for course resolution (21 values) data sets and a 0.5% cut-off for fine resolution (91 values) data sets, to identify a final list S_2 of retained

candidate parameter sets. The set S_2 represents the model parameters that produce the V_m trace closest to the measured MAP trace within the prescribed tolerances.

Signal spectral fit:

In step 2 of determining the plausible parameters, we aim to identify parameters that generate an action potential morphology that best matches the clinically measured MAP morphology. We use semi-classical signal analysis (SCSA) to perform the comparison (Reference 25). SCSA is the non-linear counterpart of the Fourier transform. We chose SCSA as it requires a limited number of modes (the negative spectrum) resulting in increased efficiency.

1. We evaluate the cost $\mathcal{S}\left(s_1^j\right)$ with the following procedure. First, we rescale the time axis within the interval [0,1] and then normalize each trace u(t) (MAP and computed V_m) as follows:

$$\hat{u}(t) = \frac{u(t) - \min(u(t \geq 35\, ms))}{max(u(t \geq 35\, ms)) - \min(u(t \geq 35\, ms))}$$

Here we consider $t \geq 35\, ms$ in the rescaling to remove artefact due to the pacing stimulus and rescale the signal to be greater than 0.

2. Next, we evaluate the Eigen-functions of the Schrödinger problem:

$$\frac{d^2}{dt^2}(\varphi) + \chi\hat{u}(t)\varphi = \lambda\varphi$$

We have discretized the problem using a pseudo-spectral method. Here the parameter χ plays the role of a parameter that increases the accuracy of $\hat{u}(t)$ by reducing the smoothness of the function. As χ gets larger, the representation is more accurate, since

the number of negative eigenvalues increases. We chose $\chi = 8000$, which adequately bounded the differences in MAP waveforms.

3. Finally, we evaluated:

$$\mathcal{S}\left(s_2^j\right) = \sum_{j=1}^{N} \frac{\left|\sqrt{-\lambda_j^C} - \sqrt{-\lambda_j^M}\right|}{\sqrt{-\lambda_j^M}}$$

Here $\lambda_j^{C,M}$ is the jth negative eigenvalue obtained from the SCSA on the computed and measured traces respectively; N is the minimum between the number of negative eigenvalues in the SCSA on the computed and clinically measured traces respectively. This provides a measure of the similarity in the shape of the two traces.

Global sensitivity analysis:

A Saltelli global sensitivity analysis (GSA) (Reference 26) of the APD values to the ionic pathway densities was performed using the data base of generated simulations, to identify variables with the greatest influence on APD. The implementation was verified against the Ishigami analytic solutions (Reference 27). GSA was not performed on SCSA due to the computational cost. We found that APD values were predominantly defined by IKr, with the least contribution from SERCA (Figure 5A of main manuscript).

We now considered a reduced analysis. We considered Ito due to its prominent role in phase 1, where measured MAP morphology differed between patients who died versus those who survived (Figure 4B from main manuscript). IKr was maintained due to its important in determining APD (Figure 5A from main manuscript). We cannot differentiate between NCX and

ICaL as they have similar importance (Figure 5A from main manuscript) and both cause a depolarizing current prolonging the action potential. As both NCX and ICaL are equally plausible explanations for the data we considered 2 sets of ionic pathways. Dataset 1: Ito, IKr and ICaL or Dataset 2: Ito, IKr and NCX. We repeated the analysis, described above, to identify the plausible parameter sets for these two new sets of ionic pathways. Parameter ranges for Dataset 1 and 2 are defined below.

DATASET 1*: ICaL (753,571 samples)*

	Ito (Gto)	IKr (GKr)	ICaL (pCa)
Min	0.004	0.0092	$0.2e^{-4}$
Max	0.04	0.092	$2e^{-4}$
Number of values	91	91	91

DATASET 2: *NCX (753,571 samples)*

	Ito (Gto)	Ikr (GKr)	NCX (Gncx)
Min	0.004	0.0092	$0.16\ e^{-3}$
Max	0.04	0.092	$1.6\ e^{-3}$
Number of values	91	91	91

Analysis of APD alternans

For each dataset (altered PCa or altered NCX) and for VT/VF or non-VT/VF phenotypes, we performed single cell simulations by pacing each 0D model at a fixed pacing cycle length for 320 stimuli, followed by 2 additional stimuli in which we evaluated APD60. This procedure was conducted for pacing cycle length starting at 250 ms and shortened (accelerated) progressively to 200 in increments of 5ms.

Alternans was assigned whenever APD60 in those 2 beats differed by > 50 ms. For each cell model, we quantified alternans as the percentage of pacing trials that exhibited alternans at slow rates (paced cycle lengths ≥ 220 ms) or at fast rates (< 220 ms). The presence of APD alternans at slower rates indicates that it arises from a lesser perturbation, which may indicate a greater vulnerability to arrhythmia (Reference 44).

We found that cell models with higher I_{CaL} more often presented APD alternans at slow rates (cycle lengths 220-235 ms) than models with lower I_{CaL}, with similar prevalence at faster rates (cycle lengths 200-215 ms). Conversely, the prevalence of APD alternans was similar between cell models with enhanced versus non-enhanced NCX for slower or faster rates.

Online Tables:

Online Table I

Layer	Parameters
Conv1D	filters = 32, kernel_size = 16, strides = 1
BatchNormalization	None
Activation	activation = 'relu'
Dropout	0.3
MaxPooling1D	pool_size=2, strides = 1
Conv1D	filters = 64, kernel_size = 16, strides = 1
BatchNormalization	None
Activation	activation = 'relu'
Dropout	0.3
MaxPooling1D	pool_size=2, strides = 1
Bidirectional (layers.LSTM)	units = 128, dropout = 0.2, recurrent_dropout = 0.3
Dense	units = 1, activation = 'sigmoid'

Online Table I Convolutional Neural Network architecture with parameters and descriptions of each layer.

Online Table II – Test characteristics at the beat-level, for all MAPs across all 10 k-cross validation sets results from CNN model and SVM model.

	Mortality				
	Accuracy	**Sensitivity**	**Specificity**	**NPV**	**PPV**
SVM	75.4%	60.0%	81.6%	83.4%	57.0%
CNN	70.6%	11.7%	94.6%	72.5%	46.8%

	VT/VF				
	Accuracy	**Sensitivity**	**Specificity**	**NPV**	**PPV**
SVM	83.2%	72.6%	89.0%	85.6%	78.2%
CNN	56.7%	40.3%	65.6%	66.9%	39.0%

Online Table III - Baseline Characteristics of Population Split by all-cause mortality at 3-years

	All Subjects (n=42)	Death (n=14)	No Death (n=28)	p
Age, y	64.7 ± 13.0	71.5 ± 8.5	61.3 ± 13.6	0.014
Gender, M/F	41/1	14/0	27/1	1
LVEF, %	27.0 ± 7.6	27.5 ± 7.4	26.70 ± 7.8	0.766
QRS Duration, ms	126 ± 33	121 ± 19.9	129 ± 38	0.495
LBBB, % (n)	28.6 (12)	23.1 (3)	31.0 (9)	0.716
RBBB, % (n)	14.3 (6)	14.3 (2)	14.3 (4)	1
IVCD, % (n)	21.4 (9)	30.8 (4)	17.2 (5)	0.437
Any IVCD, % (n)	64.3 (27)	62.1 (18)	69.2 (9)	1
Myocardial Infarct, % (n)	88.1 (37)	100 (14)	82.1 (23)	0.151
Days from MI to EPS (IQR)	3036 (1319-7015)	2248 (1270-3036)	6550 (1260-7555)	0.154
Days from revasc. to EPS (IQR)	2495 (1260-4714)	2248 (1449-3873)	2529 (903-6372)	0.658
CAD Vessels, % (n)				
LAD	59.5 (25)	69.2 (9)	55.2 (16)	0.73
LCx	54.8 (23)	61.5 (8)	51.7 (15)	1
RCA	61.9 (26)	61.5 (8)	62.1 (18)	1
Hypertension, % (n)	19.0 (8)	7.1 (1)	0.25 (7)	0.233
Diabetes Mellitus, % (n)	14.3 (6)	7.1 (1)	17.9 (5)	0.645
Laboratory values				
BNP, pg/ml (median, IQR)	341 (157–999)	900 (326.25-1325)	277 (109-502)	0.014
Sodium, mmol/L	139 ± 3.6	138 ± 4.2	139 ± 3.3	0.915
Potassium, mmol/L	4.3 ± 0.4	4.2 ± 0.4	4.4 ± 0.4	0.109
Magnesium, mmol/L	2.0 ± 0.4	2.2 ± 0.2	2.0 ± 0.4	0.134
Prior Medications, % (n)				
Beta-Blocker	78.6 (31)	72.9 (6)	89.3 (25)	0.002
ACE inhibitors/ARB	92.9 (39)	85.7 (12)	96.4 (27)	0.254
Spironolactone	19.0 (8)	14.3 (2)	21.4 (6)	697
CCB	14.3 (6)	21.4 (3)	10.7 (3)	0.383
Digoxin	38.1 (16)	31.4 (3)	46.4 (13)	0.18
Amiodarone	9.5 (4)	14.3 (2)	7.1 (2)	0.59
Statins	71.4 (30)	78.6 (11)	67.9 (19)	0.719
Implantable Device at EPS*	85.7 (36)	92.3 (12)	82.8 (24)	1

*within 14 days

Key: All patients had electrophysiology study based on the presence of ischemic cardiomyopathy, left ventricular ejection fraction ≤40% and non-sustained VT/VF (ref 18 in main manuscript). Values are n, mean ± standard deviation, or median (interquartile range). Categorical variables are compared using Fisher's exact test; continuous variables using the t-test (except BNP: Mann-Whitney U test performed because data is not normally distributed). ACE, angiotensin converting enzyme; ARB, angiotensin receptor blockers; BNP, B-type natriuretic peptide concentration; CCB, calcium channel blockers; CAD, coronary artery disease; EPS, electrophysiology study; IVCD, intraventricular conduction delay; LAD, left anterior descending artery; LBBB, left bundle branch block; LCx, left circumflex artery; MI, myocardial infarction; RBBB, right bundle branch block; RCA, right coronary artery, Revasc., coronary revascularization; Statins, HMG-CoA reductase inhibitors.

Online Table IV - Baseline Characteristics of Population Split by Inducibility of VT or VF in EPS

	All Subjects (n=42)	Induced VT/VF (n=14)	VT/VF Not Induced (n=28)	p
Age, y	64.7 ± 13.0	67.2 ± 13.1	63.4 ± 12.9	0.379
Gender, M/F	41/1	14/0	27/1	1
LVEF, %	27.0 ± 7.6	27.4 ± 10.0	26.8 ± 6.2	0.831
QRS Duration, ms	126 ± 33	123 ± 29	127 ± 36	0.761
LBBB, % (n)	28.6 (12)	28.6 (4)	28.6 (8)	1
RBBB, % (n)	14.3 (6)	14.3 (2)	14.3 (4)	1
IVCD, % (n)	21.4 (9)	28.6 (4)	17.9 (5)	0.437
Any IVCD, % (n)	64.3 (27)	71.4 (10)	60.7 (17)	0.484
Myocardial Infarct, % (n)	88.1 (37)	92.9 (13)	85.7 (24)	0.65
Days from MI to EPS (IQR)	3036 (1319-7015)	2666 (1535-6395)	2450 (1591-3598)	0.612
Days from revasc. to EPS (IQR)	2495 (1260-4714)	2450 (1591-3597)	3160 (775-5071)	0.763
CAD Vessels, % (n)				
LAD	59.5 (25)	64.3 (9)	57.1 (16)	0.73
LCx	54.8 (23)	57.1 (8)	53.6 (15)	1
RCA	61.9 (26)	71.4 (10)	57.1 (16)	0.316
Hypertension, % (n)	19.0 (8)	0 (0)	28.6 (8)	0.037
Diabetes Mellitus, % (n)	14.3 (6)	0 (0)	21.4 (6)	0.083
Laboratory values				
BNP, pg/ml (median, IQR)	341 (157–999)	490.5 (288-1433)	270 (221-721)	0.104
Sodium, mmol/L	139 ± 3.6	138 ± 4.1	139 ± 3.3	0.915
Potassium, mmol/L	4.3 ± 0.4	4.4 ± 0.5	4.4 ± 0.4	0.949
Magnesium, mmol/L	2.0 ± 0.4	2.1 ± 0.2	2.0 ± 0.4	0.34
Prior Medications, % (n)				
Beta-Blocker	78.6 (31)	64.3 (9)	78.6 (22)	0.459
ACE inhibitors/ARB	92.9 (39)	85.7 (12)	96.4 (27)	0.254
Spironolactone	19.0 (8)	35.7 (5)	10.7 (3)	1
CCB	14.3 (6)	21.4 (3)	10.7 (3)	0.383
Digoxin	38.1 (16)	92.9 (13)	10.7 (3)	0.18
Amiodarone	9.5 (4)	14.3 (2)	7.1 (2)	0.59
Statins	71.4 (30)	71.4 (20)	71.4 (10)	1
Implantable Device at EPS*	85.7 (36)	85.7 (12)	85.7 (24)	1

*within 14 days

Key: Values are n, mean ± standard deviation, or median (interquartile range). Categorical variables are compared using Fisher's exact test; continuous variables using the t-test (except BNP: Mann-Whitney U test performed because data is not normally distributed). All patients had electrophysiology study based on the presence of ischemic cardiomyopathy, left ventricular ejection fraction ≤ 40% and non-sustained VT/VF. ACE, angiotensin converting enzyme; ARB, angiotensin receptor blockers; BNP, B-type natriuretic peptide concentration; CCB, calcium channel blockers; CAD, coronary artery disease; EPS, electrophysiology study; IVCD, intraventricular conduction delay; LAD, left anterior descending artery; LBBB, left bundle branch block; LCx, left circumflex artery; MI, myocardial infarction; RBBB, right bundle branch block; RCA, right coronary artery, Revasc., coronary revascularization; Statins, HMG-CoA reductase inhibitors.

Online Table V.

Top 40 Extracted Features for endpoint of VT/VF used in the SVM model

Feature	Ampli-tude	VT/VF	Description	Category
1	1.738	time_reversal_asymmetry_statistic__lag_3	Direction reversal, i.e. vectorial change, at 3ms	Time
2	1.440	spkt_welch_density__coeff_5	Cross power spectral density at 5 frequencies	Frequency
3	-1.068	agg_linear_trend__f_agg_"min"__chunk_len_50__attr_"rvalue"	Correlation of linear trend across minima of all 50ms chunks	Time
4	1.038	change_quantiles__f_agg_"mean"__isabs_False__qh_0.8__ql_0.4	Absolute consecutive change between 0.4 and 0.8 of amplitude	Time
5	1.007	variance_larger_than_standard_deviation	Is variance larger than SD? (Boolean 1/0)	Time
6	-0.956	last_location_of_minimum	Last time point of minimum value	Time
7	0.891	agg_linear_trend__f_agg_"var"__chunk_len_10__attr_"rvalue"	Correlation of linear trend across variance of all 10ms chunks	Time
8	0.848	number_peaks__n_3	Number of peaks greater than 3 ms	Time
9	0.803	fft_coefficient__coeff_48__attr_"abs"	Absolute value of Fourier coefficient at 130Hz	Frequency (High)
10	-0.740	change_quantiles__f_agg_"mean"__isabs_True__qh_0.8__ql_0.6	Absolute consecutive change between 0.6 and 0.8 of amplitude	Time
11	-0.719	agg_linear_trend__f_agg_"var"__chunk_len_50__attr_"rvalue"	Correlation of linear trend across variance of all chunks of data of duration 50 ms	Time
12	-0.649	fft_coefficient__coeff_61__attr_"abs"	Absolute value of the Fourier coefficient at 165Hz	Frequency (High)
13	-0.639	index_mass_quantile__q_0.8	Time point of 0.8 of cumulative mass	Time
14	0.618	fft_coefficient__coeff_41__attr_"abs"	Absolute value of the Fourier coefficient at 111Hz	Frequency (High)
15	-0.546	agg_linear_trend__f_agg_"var"__chunk_len_5__attr_"slope"	Slope of linear trend across variance of all chunks of data of duration 50 ms	Time
16	-0.524	percentage_of_reoccurring_values_to_all_values	Percentage of recurring values	Time
17	0.517	large_standard_deviation__r_0.150000000000000002	Boolean is SD > 0.15 range	Time
18	0.510	fft_coefficient__coeff_20__attr_"angle"	Angle value of the Fourier coefficient at 54Hz	Frequency (Mid)
19	-0.482	change_quantiles__f_agg_"var"__isabs_False__qh_0.8__ql_0.4	Variance between 0.4 and 0.8 of magnitude	Time
20	0.425	fft_coefficient__coeff_98__attr_"imag"	Imaginary part of the Fourier coefficient at 264Hz	Frequency (High)

Feature	Ampli-tude	VT/VF	Description	Category
21	-0.422	has_duplicate_min	Boolean is minimum repeated	Time
22	-0.360	energy_ratio_by_chunks__num_segments_10__segment_focus_8	Energy in chunk 8 of 10 vs. entire series	Time
23	0.356	fft_coefficient__coeff_19__attr_"imag"	Imaginary part of the Fourier coefficient at 51Hz	Frequency (Mid)
24	-0.355	fft_coefficient__coeff_8__attr_"real"	Real part of the Fourier coefficient at 265Hz	Frequency (High)
25	0.347	approximate_entropy__m_2__r_0.1	Approximate entropy across 2ms fitered at 0.1	Frequency
26	-0.346	fft_coefficient__coeff_27__attr_"angle"	Angle value of the Fourier coefficient at 73Hz	Frequency (Mid)
27	0.343	partial_autocorrelation__lag_2	Partial autocorrelation at 2ms	Time
28	-0.317	fft_coefficient__coeff_37__attr_"real"	Real part of the Fourier coefficient at 100Hz	Frequency (Mid)
29	0.316	friedrich_coefficients__m_3__r_30__coeff_1	Friedrich coefficient 1 of 3-degree polynomial across 30 quantiles	Time
30	0.309	cwt_coefficients__widths_(2, 5, 10, 20)__coeff_14__w_5	Continuous wavelet transform for 5ms among 2, 5, 10, and 20ms	Time
31	0.300	fft_coefficient__coeff_12__attr_"real"	Real part of the Fourier coefficient at 32Hz	Frequency (Low)
32	0.300	fft_coefficient__coeff_43__attr_"angle"	Angle value of the Fourier coefficient at 116Hz	Frequency (High)
33	-0.285	fft_coefficient__coeff_38__attr_"real"	Real part of the Fourier coefficient at 103Hz	Frequency (High)
34	-0.276	large_standard_deviation__r_0.35000000000000003	Boolean is SD > 0.35 range	Time
35	-0.250	cwt_coefficients__widths_(2, 5, 10, 20)__coeff_3__w_2	Continuous wavelet transform for 2ms among 2, 5, 10, and 20ms	Time
36	0.242	fft_coefficient__coeff_25__attr_"angle"	Angle value of the Fourier coefficient at 68Hz	Frequency (Mid)
37	-0.239	fft_coefficient__coeff_28__attr_"angle"	Angle value of the Fourier coefficient at 76Hz	Frequency (Mid)
38	-0.236	change_quantiles__f_agg_"mean"__isabs_True__qh_0.2__ql_0.0	Absolute consecutive change between 0.0 and 0.2 of amplitude	Time
39	0.227	fft_coefficient__coeff_94__attr_"real"	Real part of the Fourier coefficient at 254Hz	Frequency (High)
40	-0.218	fft_coefficient__coeff_29__attr_"angle"	Angle value of the Fourier coefficient at 78Hz coefficient	Frequency (Mid)

Key: Frequency descriptions are subdivided into low bandwidth (<50 Hz), corresponding to MAP waveform shape and resting potential, high bandwidth (>100 Hz), corresponding to transients such as Phase 0 and 1, and mid- bandwidth (51-100 Hz).

Online Table VI

Top 40 Extracted Features for endpoint of all-cause mortality used in the SVM model

Feature	Ampli-tude	Death	Description	Category
1	-2.876	approximate_entropy__m_2__r_0.1	Approximate entropy across 2ms filtered at 0.1	Frequency (Low)
2	-1.798	ratio_beyond_r_sigma__r_2	Ratio of values > 2SD	Time
3	-1.750	agg_autocorrelation__f_agg_"median"__maxlag_40	Autocorrelation of medians at lags up to 40ms	Time
4	1.152	time_reversal_asymmetry_statistic__lag_3	Direction reversal at 3ms	Time
5	-0.963	spkt_welch_density__coeff_2	Cross power spectral density at 2 frequencies	Frequency
6	-0.700	agg_linear_trend__f_agg_"var"__chunk_len_50__attr_"rvalue"	Correlation of linear trend across variance of all 50ms chunks	Time
7	-0.669	change_quantiles__f_agg_"var"__isabs_False__qh_0.4__ql_0.0	Absolute consecutive variance change between 0.0 and 0.4 of amplitude	Time
8	0.656	fft_coefficient__coeff_98__attr_"abs"	Absolute value of the Fourier coefficient at 265Hz	Frequency (High)
9	0.655	large_standard_deviation__r_0.2	Boolean is SD > 0.20 range	Time
10	-0.640	ratio_beyond_r_sigma__r_1.5	Ratio of values > 1.5SD	Time
11	-0.606	number_peaks__n_3	Number of peaks greater than 3 ms left or right	Time
12	0.573	fft_coefficient__coeff_23__attr_"real"	Real part of the 23Fourier coefficient at 62Hz	Frequency (Mid)
13	0.555	ar_coefficient__k_10__coeff_0	Autoregression coefficient max lag = 10	Time
14	-0.537	fft_coefficient__coeff_37__attr_"real"	Real part of the Fourier coefficient at 100Hz	Frequency (High)
15	-0.488	agg_linear_trend__f_agg_"var"__chunk_len_5__attr_"rvalue"	Correlation of linear trend across variance of all 5ms chunks	Time
16	0.446	agg_linear_trend__f_agg_"max"__chunk_len_50__attr_"rvalue"	Correlation of linear trend across maximums of all 5ms chunks	Time
17	-0.307	fft_coefficient__coeff_28__attr_"angle"	Angle value of the Fourier coefficient at 76Hz	Frequency (Mid)
18	-0.287	energy_ratio_by_chunks__num_segments_10__segment_focus_7	Energy in chunk 7 of 10 vs. entire series	Frequency (Mid)
19	-0.286	agg_linear_trend__f_agg_"min"__chunk_len_50__attr_"slope"	Slope of linear trend across minimum of all 50ms chunks	Time
20	0.283	fft_coefficient__coeff_8__attr_"real"	Real part of the Fourier coefficient at 22Hz	Frequency (Low)

Feature	Ampli-tude	Death	Description	Category
21	0.277	fft_coefficient__coeff_46__attr_"angle"	Angle value of the Fourier coefficient at 14Hz	Frequency (Low)
22	0.249	fft_coefficient__coeff_2__attr_"imag"	Imaginary party of the Fourier coefficient at 5.4Hz	Frequency (Low)
23	-0.236	binned_entropy__max_bins_10	Entropy max in up to 10 bins	Frequency (High)
24	0.232	fft_coefficient__coeff_5__attr_"angle"	Angle value of the Fourier coefficient at 13.5Hz	Frequency (Low)
25	0.225	cwt_coefficients__widths_(2, 5, 10, 20)__coeff_13__w_5	Continuous wavelet transform for 5ms among 2, 5, 10, and 20ms	Time
26	-0.215	cwt_coefficients__widths_(2, 5, 10, 20)__coeff_10__w_2	Continuous wavelet transform for 2ms among 2, 5, 10, and 20ms	Time
27	0.205	change_quantiles__f_agg_"mean"__isabs_True__qh_1.0__ql_0.8	Absolute consecutive mean change between 0.8 and 1.0 of amplitude	Time
28	-0.205	fft_coefficient__coeff_78__attr_"abs"	Absolute value of the Fourier coefficient at 211Hz	Frequency (High)
29	0.202	fft_coefficient__coeff_64__attr_"angle"	Angle value of the Fourier coefficient at 173Hz	Frequency (High)
30	-0.200	fft_coefficient__coeff_82__attr_"angle"	Angle value of the Fourier coefficient at 222Hz	Frequency (High)
31	0.197	longest_strike_above_mean	Length of longest string above mean	Time
32	-0.193	large_standard_deviation__r_0.15000000000000002	Boolean is SD > 0.15 range	Time
33	0.191	last_location_of_maximum	Last time point of maximum	Time
34	-0.191	sum_of_reoccurring_data_points	Sum of all recurring data points	Time
35	0.189	fft_coefficient__coeff_42__attr_"angle"	Angle value of the Fourier coefficient at 114Hz	Frequency (High)
36	0.174	fft_coefficient__coeff_79__attr_"real"	Real part of the Fourier coefficient at 214Hz	Frequency (High)
37	0.173	energy_ratio_by_chunks__num_segments_10__segment_focus_9	Energy in chunk 9 of 10 vs. entire series	Time
38	-0.166	fft_coefficient__coeff_29__attr_"angle"	Angle value of the Fourier coefficient at 78Hz	Frequency (Mid)
39	0.165	value_count__value_0	Number of 0 values	Time
40	0.162	has_duplicate_min	Boolean is minimum duplicated	Time

Key: Frequency descriptions are subdivided into low bandwidth (<50 Hz), corresponding to MAP waveform shape and resting potential, high bandwidth (>100 Hz), corresponding to transients such as Phase 0 and 1, and mid- bandwidth (51-100 Hz).

Online Table VII – Confusion matrices for all single-beat MAPs across all 10 test sets

VT/VF

	Percent	95% Conf. Intervals Lower	Upper
Sensitivity	72.65	71.49	73.78
Specificity	88.98	88.38	89.56
PPV	78.24	77.12	79.32
NPV	85.65	84.98	86.29
Accuracy	83.22	82.64	83.78

Mortality

	Percent	95% Conf. Intervals Lower	Upper
Sensitivity	59.95	58.54	61.35
Specificity	81.64	80.92	82.34
PPV	57.03	55.64	58.41
NPV	83.38	82.68	84.05
Accuracy	75.37	74.71	76.03

Online Table VIII - Similar Respiratory Rate for MAPs predicting/not predicting each endpoint

	VT/VF	No VT/VF	Mort	No Mort
Respiratory Rate	14.71	15.45	15.59	14.94
Standard deviation	2.87	3.00	2.99	2.95
t-test p	0.45		0.49	

Online Table IX - Similar recording quality, measured as the peak of autocorrelation for successive beats, for MAPs predicting/not predicting each endpoint

	VT/VF	No VT/VF	Mortality	No Mortality
MAP consistency by autocorrelation	0.89	0.86	0.86	0.88
Standard deviation	0.09	0.08	0.09	0.09
t-test p	0.41		0.57	

Supplemental Figures:

Online Figure I

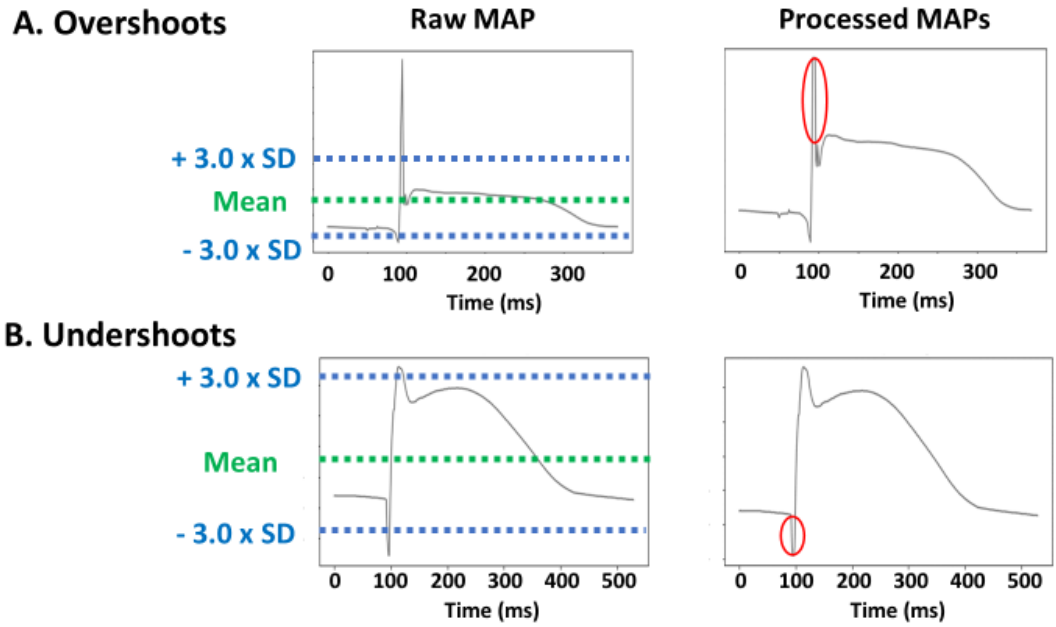

Online Figure I. Preprocessing Applied to MAPs. A. Clipping phase 0 overshoot, in an RV MAP from a 67-year-old male with LVEF 25%. Outlier removal eliminated this phase 0 overshoot while maintaining MAP shape. B. Clipping undershoot from a Ventricular MAP in a 59-year-old male with LVEF 10%. The negative undershoot just before phase 0, possibly related to pacing artifact, was attenuated by this uniform approach to outlier removal. Results from the analysis did not change qualitatively if this step was omitted.

Online Figure II

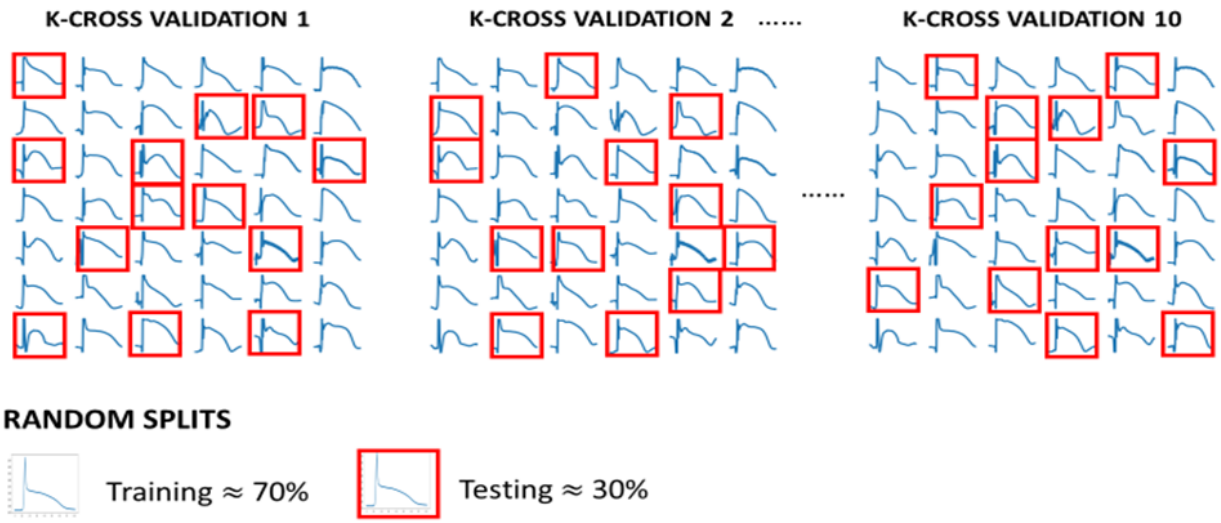

Online Figure II. K=10 Cross Validations Used in Study. Each panel shows a single MAP from each patient (N=42) to represent the set of all recordings from that patient. Data were randomly allocated into either training (unboxed) or test (red boxes) cohorts, with all beats from each patient allocated together (stratified Monte Carlo cross-validation). This process was repeated for 10 cross-validation splits. In each split, approximately 70% of beats were used for training and 30% were reserved for testing. Training and testing data were distinct for each K-cross validation split.

Online Figure III

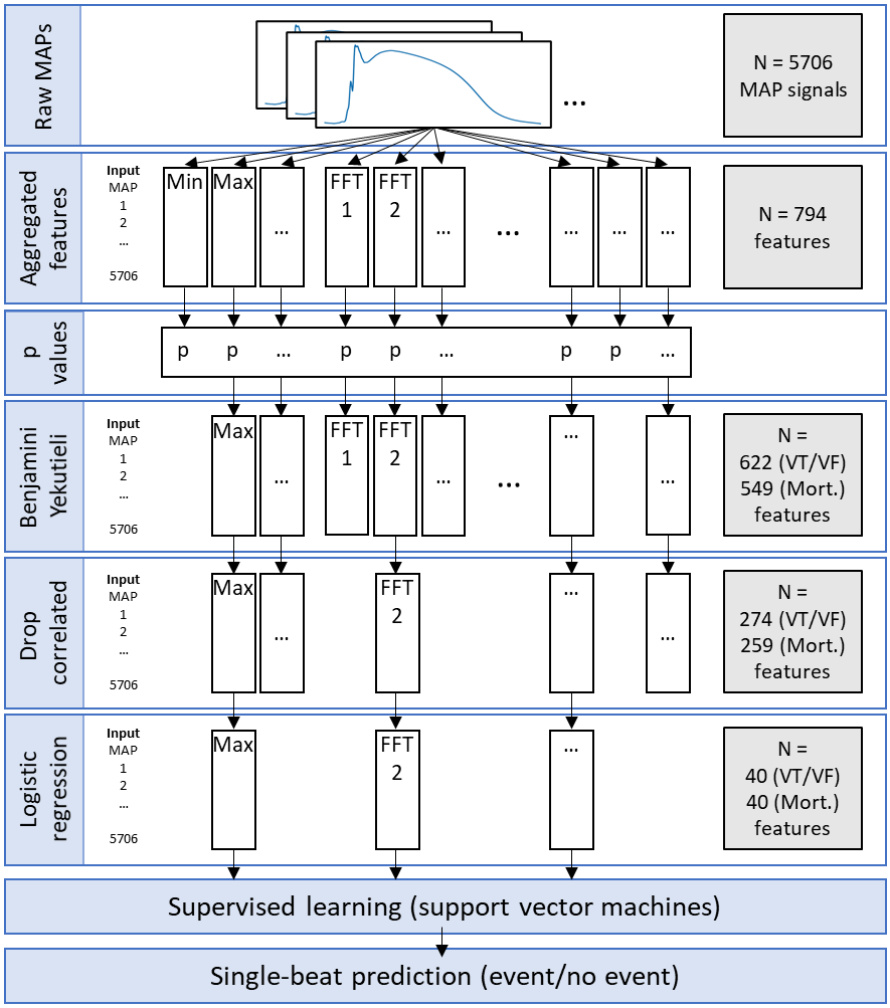

Online Figure III. Calculation and selection of features for supervised learning – Raw MAP signals (N = 5706) are analyzed using the Python tsfresh package to calculate 794 features for each single-beat recording. Each calculated feature is assigned a p value according to the outcome label (VTVF or mortality) and filtered using the Benjamini Yekutieli procedure (resulting in 622 and 549 features, respectively. When features correlate highly to each other, all but the feature with the highest p-value is removed to result in 274 and 259 features. The top 40 features selected by logistic regression optimized prediction in training and were input to the supervised learning (SVM) model for each endpoint.

300

Online Figure IV

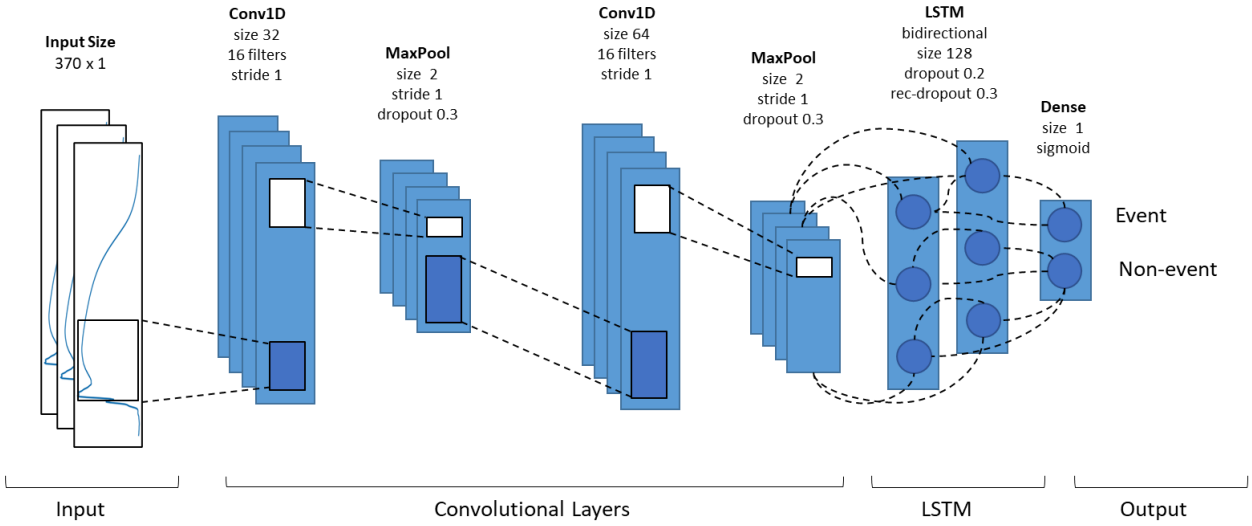

Online Figure IV. CNN model architecture – CNN model, on input size of 370 samples for a single-beat MAP, with two convolutional layers and a bidirectional long-short term memory (LSTM) layer that classified events (VT/VF or mortality) vs. non-events (arrhythmia-free or survival)

Glossary of Terms

Computational phenotyping - Computational phenotypes are disease phenotypes, identified in this case from machine learning of clinically measured ventricular action potentials coupled with computational cell models, which indicate a high or low risk of clinical events (here, ventricular arrhythmias or death on long-term follow-up).

tsfresh - *tsfresh* is a library of mathematical time-series parameters that efficiently represents time and frequency-based features for supervised learning. To produce features using tsfresh, the voltage time series data from MAP recordings are passed into the functions of the library and scalar values are returned for each of 794 features. These are ranked based on p-values for each output label in turn, and those with least significant features are removed by the Benjamini-Yekutieli procedure. Resulting features are further filtered as inputs for supervised learning.[1]

Features – Features are mathematical descriptions of an input signal or image described by a value, function, or pattern that can be used as inputs to supervised learning models.

Parameter sets – Parameter sets are the group of channel conductance values that are used for a given state of the O'Hara Rudy model simulation. Each parameter set contains 5 values corresponding to the 5 channels evaluated in this work.

L1 regularization, regularization factor, 'liblinear' solver – L1 regularization, regularization factor, and the 'liblinear' solver are parameters of the linear regression model used to choose the top 40 features that correlated with the endpoints.

Scikit-learn library – A python library containing various classification, regression, and clustering algorithms for data science applications.

ReadMe Document for Source Code and Demo

1. Background

This document provides readme documentation for the source code used to generate the results for the manuscript entitled "Machine Learning of in vivo Tissue Electrophysiology in Patients with Heart Failure ".

There is also a demo code to show the results of the trained model for a sample dataset.

2. Files attached

- Code: The main code is presented in a Jupyter notebook format (.ipynb). The code provides information for all the steps and the functions that are used in the result. Comments are provided for each function.
    - The main code is saved in "Code_for_manuscript_submission.ipynb" as jupyter notebook in the Code folder. The rest of the functions are helper functions saved as a .py file. The full source code will only run with full dataset (we only provide demo dataset).
- Data: Only a subset of the data is provided for demo purposes and can be found in the Demo folder.
- Demo Folder contents:
    - 20191219 is an excel sheet showing the actual labels for both VTVF and Mortality endpoints and whether they were in training/validation splits in the trained model
    - Calc_metrics_v2: helper function to calculate accuracy, sensitivity, specificity, NPV, PPV.
    - Demo_Code.ipynb: Jupyter notebook to run demo. Running this demo will show results from the sample dataset provided.
    - Mortality_CV1_finalized_mode.sav: trained model using cross validation 1 for mortality endpoint.
    - VTVF_CV1_finalized_model.sav: trained model using cross validation 1 for VTVF endpoint.
    - Mortality_labels_demo & Mortality_tsfresh_features_demo: input and true output for model (Mortality). First 5-digit contain patient ID, and last 4 digits contain beat ID.
    - VTVF_labels_demo & VTVF_tsfresh_features_demo: input and true output for model (VTVF).
    - demo_data_20191219.npz: numpy (.npz) file that has the voltage-timeseries MAPs. Each point is 1msec apart and the values are voltages in mV.

3. Hardware and Software

This program runs on a desktop computer system with following specifications:

- Inter Core i9-9900K CPU @3.6Ghz, 3600 Mhz, * cores, 16 Logical Processors
- Microsoft Windows 10 Pro

- 32 GB RAM

All computations were performed on Python 3.6 using Anaconda Navigator 1.9.7. The following packages were used:

- numpy 1.17.3
- pandas 0.23.4
- pandas-datareader 0.8.0
- scikit-learn 0.21.3
- scipy 1.3.1
- tsfresh 0.12.0
- xlrd 1.2.0
- xlsxwriter 1.2.6
- jupyter 1.0.0
- pickle 1.0 or higher
- matplotlib 3.3.0

4. Time to execute

All runtimes are based on the hardware specifications provided in section 3. Most commands run in less than 1 minute and a few take up to 3 minutes. The only part that takes a considerable time (~15 minutes) is "extract_features_without_label" which extracts all the tsfresh features. This command is performed in the "Code_for_manuscript_submission.ipynb" Jupyter file under section "Feature extraction using tsfresh" (this requires the full dataset to run. Only code is provided).

5. Instructions to run

1. If downloaded as a zipped folder, you will need to unzip the folder.
2. You will need to install the packages listed in section 3.
3. Running every cell in the Demo Jupyter file notebook in order will run the program and produce the results in the Jupyter notebook.
4. The Demo also allows to plot different MAP beats for the demo files (can be configured). The runtime for the demo file takes a few minutes or less (tested on machine with specifications in section 3, but it should run fast on any modern machine as well).

6. Software License